

**1            Remote Sensing Methods for Identifying Ephemeral  
2            Water Bodies Across Arizona**

**3            Travis Zalesky<sup>1</sup>**

**4            <sup>1</sup>University of Arizona,**

5      **Abstract**

6      A variety of remote sensing methods are investigated for their ability to detect  
 7      ephemeral water bodies across the state of Arizona. The strengths and weaknesses of  
 8      each are discussed.

9      **Plain Language Summary**

10     Results and methods for detecting transient water bodies using satellite data.

11     **1 Introduction**

12     As part of the Arizona Tri-University Recharge (ATUR) project, multiple methods  
 13    for identifying and quantifying ephemeral water bodies across the state of Arizona  
 14    (AZ) have been investigated. For reasons that will be discussed, accurate identifi-  
 15    cation of ephemeral, or temporary, water bodies is a challenge, and efforts to-date  
 16    have shown limited success. Methods, results, and challenges are discussed, and  
 17    potential paths forward shall be explored.

18     Ephemeral water bodies are common features in the arid American southwest. Typ-  
 19    ically very shallow, these water bodies range in size from a few cm rock pools to  
 20    sheet flow associated with flash floods, and playas up to several km in diameter  
 21    (Crawford, 1981; Whitford & Duval, 2020). While playas and intermittent streams  
 22    are well mapped across AZ, there is no consensus on the volume of water which  
 23    flows through these systems. More to the point, there is no widely accepted estimate  
 24    of the volume of water which either evaporates or recharges from these internally  
 25    draining basins.

26     It is not clear what fraction of water which flows onto a playa is evaporated vs. recharged.  
 27    On the one hand, the nature of playas results in the slow accumulation of surface  
 28    salts and fine sediments (clays and silts), which are generally impervious and detri-  
 29    mental to infiltration and subsequent recharge (Whitford & Duval, 2020). Addi-  
 30    tionally, playas may be an oasis for drought resistant flora, increasing local evapo-  
 31    transpiration, even after shallow surface soil layers have dried out (Crawford, 1981).  
 32    Alternately, these mineral rich surface crusts may be prone to expansion when wet-  
 33    tered, and are frequently characterized by deep cracks which provide avenues for water  
 34    infiltration below the impervious layers (Whitford & Duval, 2020). While the ma-  
 35    jority of water flowing onto most playas will be lost to evaporation, there may be  
 36    specific playas where water loss by infiltration may exceed evaporation (Whitford  
 37    & Duval, 2020). At least initially, we will assume that all water flowing onto playas  
 38    shall be evaporated, subject to later reevaluation and refinement.

39     The primary target of this study is to estimate and quantify the volume of water  
 40    flowing into small to medium sized playas, on the order of ~500 m to ~10 km in  
 41    diameter, although identification of sheet flow may also be incidental. The general  
 42    method outlined is to use remote sensing technology to identify standing water  
 43    broadly across the study area, across a time series. By identifying standing water,  
 44    and assuming a constant water depth, water volume can be estimated. Additionally,  
 45    an approximation of “continuously wetted” days can provide an initial estimate  
 46    of evaporation rates, and through comparison with alternate evapotranspiration  
 47    estimates, may be useful for estimating infiltration rate (e.g. if water loss rate is 2  
 48    cm/day and the evapotranspiration rate is 1.5 cm/day then the implied infiltration  
 49    rate would be 0.5 cm/day).

50     The study area used for method development is primarily Hualapai (pronounced  
 51    “wall-a-pie”) Playa (a.k.a. Red Lake), located in northwest AZ, approx. 60 km  
 52    southeast of Lake Mead (Figure 1). This ephemeral playa is roughly 8 km in dia-  
 53    meter, and is one of the largest playas in AZ. Furthermore, local landowners surround-  
 54    ing Hualapai Playa have expressed sincere interest in our project, creating additional

55 public-relations incentives related to this particular playa. Lastly, it's proximity to  
 56 Lake Mead and Lake Mohave provide a convenient region for testing these methods  
 57 against known areas of permanent surface water. Additional playas are investigated  
 58 as needed.

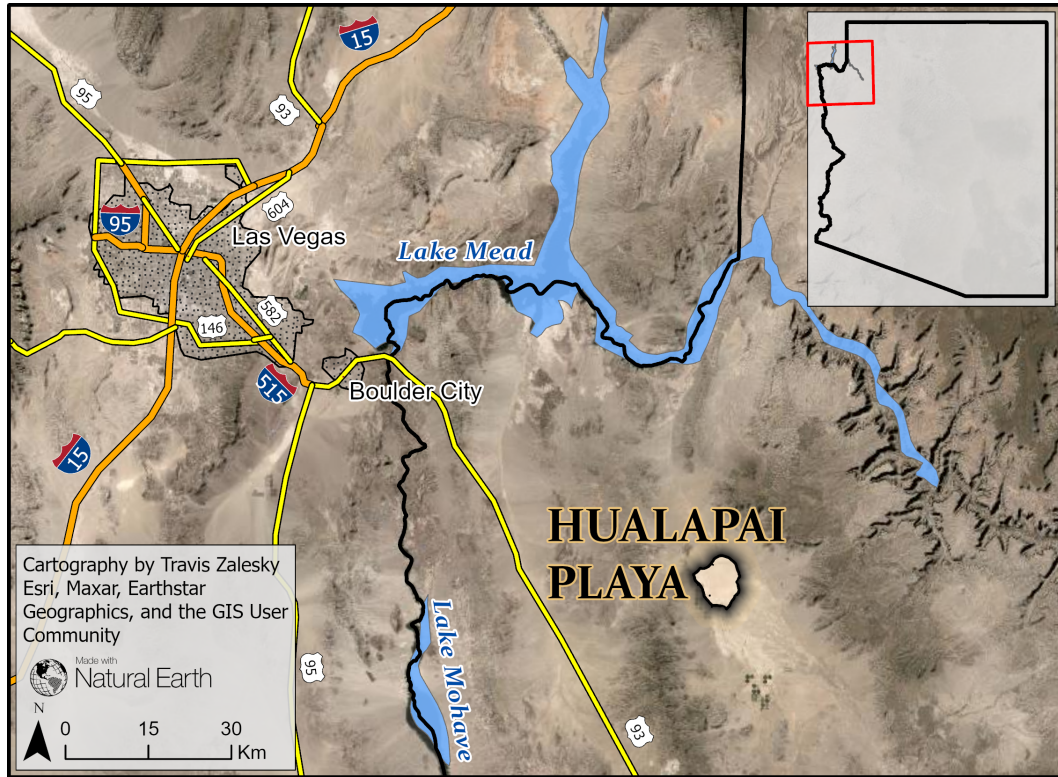


Figure 1: Hualapai Playa locator map.

59 One of the most challenging aspects of developing these methods is the lack of  
 60 quality ground-truth data. Without existing data regarding date and duration of  
 61 standing water within these ephemeral features, it is extremely difficult to validate  
 62 our methods. While reasonable assumptions can be made about method accuracy  
 63 (or inaccuracy as the case may be), any method, either those presented herein, or  
 64 future methods not yet considered, will have to be validated using a known and well  
 65 characterized ephemeral water body, ideally within AZ, or elsewhere in a similar  
 66 arid environment.

## 67 2 Methods & Results

### 68 2.1 Method 1: Otsu Thresholding with Synthetic Aperture Radar

69 Otsu thresholding is an unsupervised machine vision technique which seeks an optimal  
 70 threshold for segmenting an image into a binary classification based on a simple  
 71 histogram classification (Otsu et al., 1975). The method was initially developed in  
 72 the late '70s, and is widely applicable to a range of computer vision classification  
 73 problems. It assumes a bi-modal histogram distribution and determines an optimal  
 74 thresholding value through the integration of the histogram, rather than simply re-  
 75 lying on local histogram properties "such as valley[s]" (Otsu et al., 1975). In recent  
 76 years, Otsu thresholding has been combined with Synthetic Aperture Radar (SAR)  
 77 satellite imagery to map surface water, such as flood monitoring in the Mekong  
 78 Delta (Tran et al., 2022). The properties of surface water and SAR make an ideal

pairing for use in Otsu thresholding. The smooth surface characteristics of surface water create low SAR back-scatter, appearing as very dark pixels (Figures 2-3). Compared to the surrounding land surface, water typically has a very high contrast in SAR imagery, which can be leveraged for Otsu thresholding. Additionally, the cloud penetrating characteristics of SAR offer unparalleled all-weather monitoring capabilities.

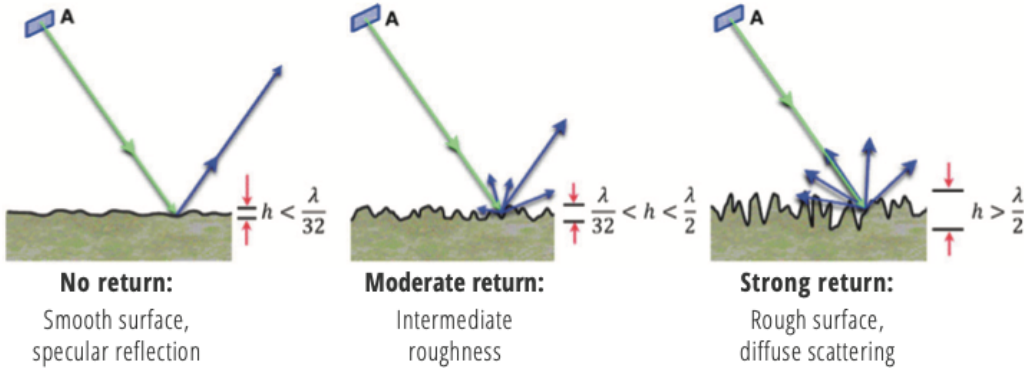


Figure 2: Synthetic Aperture Radar signal return strength (i.e. back-scatter) is a function of the roughness of the ground surface. Credit: Meyer (2019), Figure 2.8. For educational purposes only.

This method initially seemed like an ideal solution. High resolution SAR imagery is freely available from the European Space Agency (ESA) Sentinel-1 satellite, with a global coverage from late 2014 to present, and a 6-day revisit time. Google Earth Engine (GEE) code for Otsu thresholding was easily adapted from Markert et al. (2023), and preliminary results appeared to be promising. Initial analysis appeared to show surface water ponding on Hualapai Playa in mid-Jan 2020. These preliminary results were circulated internally, and purported to be both evidence of surface water, and proof-of-concept for method validation. However, further research and wider application of this method revealed two critical flaws.

Firstly, the method, as applied in GEE, was highly sensitive to the size and characteristics of any given playa. For larger playas, the method was generally suitable, but required a substantial amount of manual parameter optimization to function properly. For small to medium sized playas, the method was largely unstable, resulting in persistent errors. As a result this method is not particularly scalable, and at best could be used for a selection of the states largest playas, such as Hualapai and Willcox Dry Lake (southeast AZ).

More critically, this method is sub-optimal for arid regions, as flat sandy surfaces also result in low SAR back-scatter, appearing similar or indistinguishable from surface water. The hard-pan surface of a dry playa is particularly apt to be misidentified by this method, resulting in a high likelihood of false positives. It is currently unclear if the preliminary results purporting to have identified surface water on Hualapai Playa in Jan. 2020 are true or false positives, as there is no associated ground-truthing data against which to compare. Regardless of the truthiness of these results it is evident that this method can not be used reliably within the study area without widespread and comprehensive testing and validation of results. Given the scheduling and budgetary constraints of this project widespread survey data

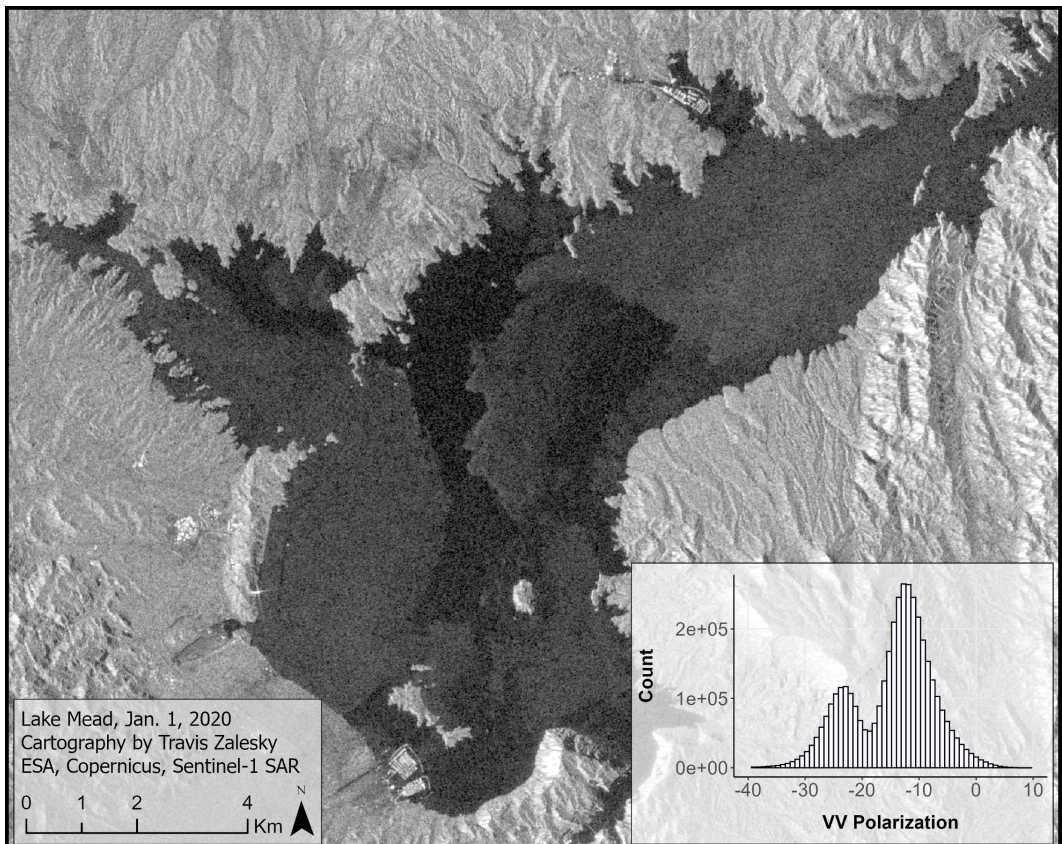


Figure 3: High resolution Synthetic Aperture Radar (SAR) imagery of Lake Mead, obtained from the European Space Agency (ESA) Sentinel-1 satellite (1-1-2020). Surface water appears dark, and contrasts strongly with the surrounding land surface, resulting in a bimodal histogram distribution, ideal for use in Otsu thresholding.

111 collection is not feasible, and while further development of this method may be  
 112 warranted (generally), it is not appropriate for our purposes. Therefore alternate  
 113 methods must be explored.

## 114 **2.2 Method 2: Normalized Difference Water Index with Landsat Multi- 115 spectral Imagery**

116 Collectively, the 9 Landsat satellites provide the longest continuous record of space-  
 117 based earth observations, from 1973 to present. Therefore, it may seem like an  
 118 obvious candidate for monitoring infrequent phenomena, such as surface water pond-  
 119 ing on playas, which may only happen once every several years (depending on the  
 120 playa). However, Landsat imagery has several disadvantages compared to SAR.  
 121 Firstly, the 30 m resolution of Landsat imagery is nine times coarser than the 10  
 122 m resolution of Sentinel-1 SAR. Second, the revisit time for Landsat satellites is  
 123 16-days, more than double that of Sentinel-1. By combining data from multiple  
 124 Landsat satellites this effective revisit time may be cut to 8-days, but this may not  
 125 be possible throughout the full time series of interest. Additionally, the visible and  
 126 infrared spectral bands used by Landsat sensors are not capable of penetrating  
 127 clouds, and while cloud-masking can be achieved through post-processing, the pres-  
 128 ence of clouds has the potential to obfuscate the phenomena of interest. Combined,  
 129 these three disadvantages compound, resulting in much sparser data availability for  
 130 Landsat imagery in comparison to Sentinel-1.

131 Furthermore, while indices for surface water monitoring utilizing Landsat spectral  
 132 bands, such as the Normalized Difference Water Index (NDWI), are widely used,  
 133 they are imprecise classifiers on their own. NDWI in particular, is suspectable to  
 134 misclassifying shadows as water. NDWI is defined as the difference between the  
 135 green and near-infrared (NIR) bands divided by the sum of the green and NIR  
 136 bands (for Landsat 8/9, bands 3 and 5 respectively; Equation 1).

$$137 \text{NDWI} = \frac{\text{Green} - \text{NIR}}{\text{Green} + \text{NIR}} \quad (1)$$

137 Despite these disadvantages, it may still be possible to characterize and quantify  
 138 ephemeral water bodies using this dataset.

139 Fortunately, Landsat data is freely available, easily accessible through GEE, and  
 140 Landsat Collection 2 datasets include post-processing data which is directly appli-  
 141 cable to this method, including cloud and cloud shadow masks, as well as a pre-  
 142 calculated water mask (which appears to be largely coincident with  $\text{NDWI} > 0$ ).  
 143 However, this water mask is over inclusive, and not suitable for use as is.

144 A large number of features identified as water in the provided Landsat water mask  
 145 layer appeared to correspond to the northward aspect of terrain features. Therefore,  
 146 to refine the provided layer by reducing the false positives resulting from natural  
 147 terrain shadows I created a hillshade (or hill shadow) layer in GEE from a high  
 148 resolution (10 m) USGS digital elevation model (DEM). For each image in the Land-  
 149 sat collection, sun angle and azimuth were obtained from the image metadata and  
 150 passed to the hillshadow function to create a custom terrain shadow mask. The pro-  
 151 vided Landsat water mask was compared against the custom terrain shadow mask,  
 152 and any purported water which overlapped a terrain shadow was removed.

153 Upon evaluation, this method worked fairly well, but still left lots of small crescent  
 154 shaped remnants of the Landsat water mask resulting from the mis-matched resolu-  
 155 tion of the imagery and the DEM. Therefore the hillshade was dilated using a local  
 156 minimum function with a 150 m (5 pixel) square neighborhood. This effectively re-  
 157 moved most of the remaining stippling and partial terrain shadows, however it also  
 158 partially clipped some known water features, for example along the southern shore  
 159 of Lake Mead. Although the accuracy has not been formally tested, visual analysis

160 appears to confirm that the removal of false positives (terrain shadows) substantially  
 161 outweighs the loss of true positives (masked water bodies).

**i Note**

This hillshadow dilation method was the first idea, and works reasonably well, with some losses of correctly identified water mask, particularly adjacent to steep terrain. An alternate strategy to reduce stippling and partial terrain shadows would be to identify and remove small features using a connected pixel count, as in the [Random Forest Flood Map](#).

162

163 This method appears to be working reasonably well, as it is consistently identifying  
 164 know bodies of water such as Lake Mead, even appearing to capture fluctuating wa-  
 165 ter levels in the lake's headwaters, while limiting the number of false positives from  
 166 terrain shadows (Figure 4). However, it still requires on the ground validation with  
 167 a known ephemeral water body. Additionally, there still remain some number of  
 168 false positives associated with large building shadows (buildings are not included in  
 169 DEMs), such as in Las Vegas, and a number of unmasked cloud shadows (Figure 5).

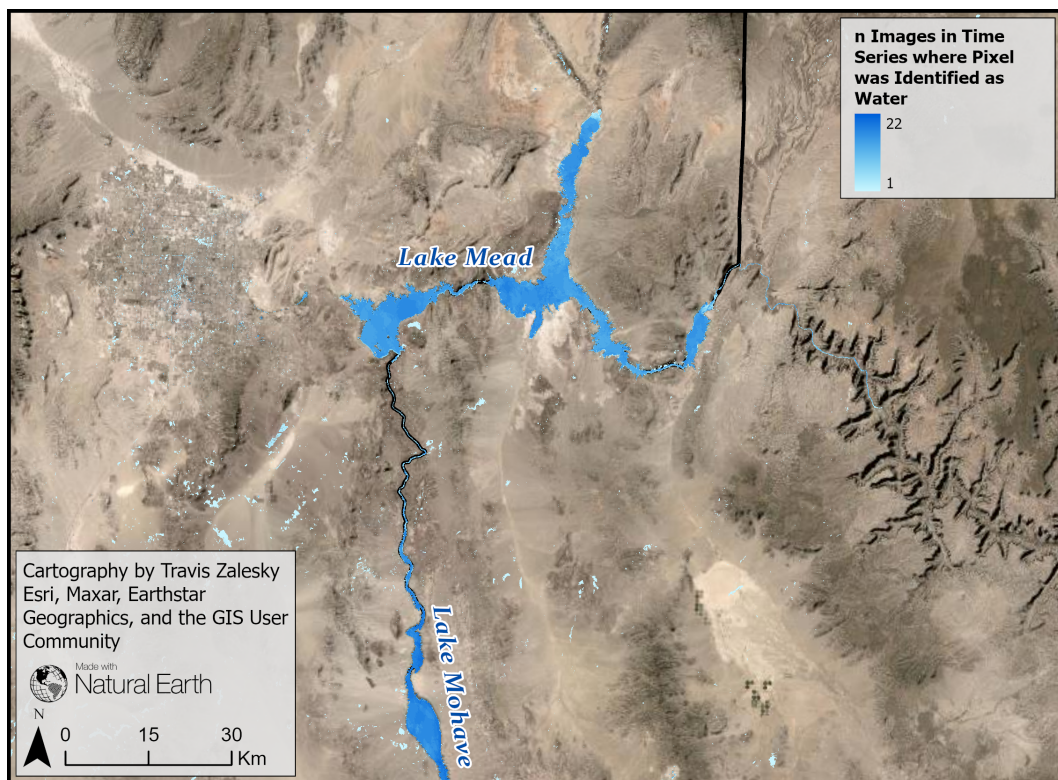


Figure 4: Time series analysis of 22 Landsat images of Lake Mead and Hualapai Playa in 2020 with potential water sources mapped in blue. The more frequently a pixel was identified as water, the more saturated the color.

170

171 Despite its limitations compared to SAR data, this Landsat method has shown enor-  
 172 mous potential. Further development of this method is warranted, and methodologi-  
 173 cal improvements are likely. However, to fully validate this method **we desperately**  
 174 **need to find Landsat images of a known ephemeral water body when**  
**flooded.** This need for a known test case to validate the method is made more

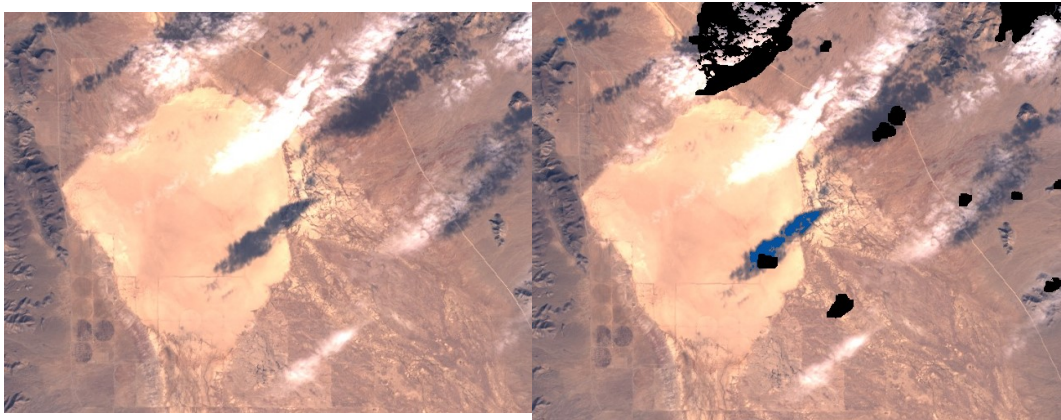


Figure 5: Google Earth Engine screen captures. A cloud moving over Hualapai Playa on 11/26/2020 cast a shadow which is only partially captured by the cloud mask (right; black), and is subsequently misclassified as water by the algorithm (right; blue).

challenging by the long revisit time of the Landsat satellites, as well as the need for clear (cloud free) conditions. **Any available historical records of known flood events on Hualapai Playa, or other large playas in the state would be enormously helpful!**

### 3 Further Recommendations

### 4 Conclusion

### References

- Crawford, C. S. (1981). Chapter 17 - the invertebrate community of ephemeral waters. In *Biology of desert invertebrates* (pp. 234–247). Springer-Verlag.
- Markert, K., Donchyts, G., & Haag, A. (2023). Chapter A2.3 surface water mapping. In J. A. Cardille, N. Clinton, M. A. Crowley, & D. Saah (Eds.), *Cloud-based remote sensing with google earth engine: Fundamentals and applications* (1st ed.). Springer Cham. [https://docs.google.com/document/d/12cwzbNXtBQnm5switfL1v1v1stnp5D5gXcQeZMP\\_iJI/edit?tab=t.0#heading=h.2gd4k88k0hkr](https://docs.google.com/document/d/12cwzbNXtBQnm5switfL1v1v1stnp5D5gXcQeZMP_iJI/edit?tab=t.0#heading=h.2gd4k88k0hkr)
- Meyer, F. (2019). Chapter 2 - spaceborne synthetic aperture radar: Principles, data access, and basic processing techniques. In A. Flores-Anderson, K. Herndon, R. Thapa, & E. Cherrington (Eds.), *The SAR handbook: Comprehensive methodologies for forest monitoring and biomass estimation*. <https://doi.org/10.25966/nr2c-s697>
- Otsu, N. et al. (1975). A threshold selection method from gray-level histograms. *Automatica*, 11(285-296), 23–27.
- Tran, K. H., Menenti, M., & Jia, L. (2022). Surface water mapping and flood monitoring in the mekong delta using sentinel-1 SAR time series and otsu threshold. *Remote Sensing*, 14(22). <https://doi.org/10.3390/rs14225721>
- Whitford, W. G., & Duval, B. D. (2020). Chapter 8 - consumers and their effects (W. G. Whitford & B. D. Duval, Eds.; pp. 203–263). Academic Press. <https://doi.org/10.1016/B978-0-12-815055-9.00008-4>